

Mammographic Parenchymal Texture as an Imaging Marker of Hormonal Activity: A Comparative Study Between Pre- and Post-Menopausal Women

Dania Daye¹, Ezra Bobo¹, Bethany Baumann¹, Antonios Ioannou¹, Emily F. Conant², Andrew D.A. Maidment² and Despina Kontos²
Department of Bioengineering¹, Department of Radiology²,
University of Pennsylvania, 3400 Spruce St., Philadelphia PA 19104
ddaye@mail.med.upenn.edu

ABSTRACT

Mammographic parenchymal texture patterns have been shown to be related to breast cancer risk. Yet, little is known about the biological basis underlying this association. Here, we investigate the potential of mammographic parenchymal texture patterns as an inherent phenotypic imaging marker of endogenous hormonal exposure of the breast tissue. Digital mammographic (DM) images in the cranio-caudal (CC) view of the unaffected breast from 138 women diagnosed with unilateral breast cancer were retrospectively analyzed. Menopause status was used as a surrogate marker of endogenous hormonal activity. Retroareolar 2.5cm² ROIs were segmented from the post-processed DM images using an automated algorithm. Parenchymal texture features of skewness, coarseness, contrast, energy, homogeneity, grey-level spatial correlation, and fractal dimension were computed. Receiver operating characteristic (ROC) curve analysis was performed to evaluate feature classification performance in distinguishing between 72 pre- and 66 post-menopausal women. Logistic regression was performed to assess the independent effect of each texture feature in predicting menopause status. ROC analysis showed that texture features have inherent capacity to distinguish between pre- and post-menopausal statuses (AUC>0.5, p<0.05). Logistic regression including all texture features yielded an ROC curve with an AUC of 0.76. Addition of age at menarche, ethnicity, contraception use and hormonal replacement therapy (HRT) use lead to a modest model improvement (AUC=0.78) while texture features maintained significant contribution (p<0.05). The observed differences in parenchymal texture features between pre- and post- menopausal women suggest that mammographic texture can potentially serve as a surrogate imaging marker of endogenous hormonal activity.

Keywords: Digital mammography, parenchymal texture pattern, hormonal activity, breast cancer risk.

1. INTRODUCTION

Breast cancer is the most commonly diagnosed malignancy of women worldwide [1] and is the second leading cause of cancer mortality in the female population [2]. Estimating a woman's risk of breast cancer is becoming increasingly important in clinical practice. As new strategies for breast cancer prevention and early detection become available, it is essential to provide accurate, clinically relevant methods for identifying women at high risk of breast cancer. Although progress has been made, no method currently exists to accurately identify high-risk women from the general population who would benefit most from such interventions. Most research to date has focused on identifying women at increased familial risk (*i.e.*, BRCA1/2 carriers) [3], which only account for the 5-10% of the incident breast cancers in the population. On the other hand, NCI's breast cancer risk assessment tool for the general population, the Gail model, has only modest discriminatory accuracy at the individual level [4].

Many studies support a relationship between mammographic texture and breast cancer risk [5-7]. Yet, the biological basis of this association is not well understood. Mammographic texture features capture the admixture of properties of the underlying epithelial and stromal breast tissue components, potentially reflecting inherent breast tissue characteristics that are related to breast cancer risk. Endogenous hormonal activity, reflected by sex steroid hormone production, is strongly associated with increased breast cancer risk and is known to affect the morphology of breast tissue. Epidemiologic evidence provides strong support for the etiologic role of endogenous hormones in breast cancer

[8-10]. With menopause, there is a drastic reduction in the amount of endogenous sex hormones produced by the body. This, in turn, affects women's risk of developing breast cancer.

As a first step towards elucidating the underlying biological association between breast cancer risk and mammographic texture patterns, we hypothesize that mammographic texture features are associated with hormonal activity and therefore can serve as an inherent phenotypic imaging marker of endogenous hormonal exposure of the breast tissue. For our study population, menopause status was used as a surrogate of endogenous hormonal activity. Identifying differences in parenchymal texture between pre- and post- menopausal women may serve as a feasibility study indicating that texture features have the potential to serve a surrogate imaging marker of endogenous hormonal activity. Our long-term hypothesis is that texture features can be incorporated into breast cancer risk estimation models to improve breast cancer risk estimation at the individual level.

2. METHODS

2.1. Dataset

Unilateral cranio-caudal (CC) digital mammographic (DM) images of the unaffected breasts from 138 women diagnosed with breast cancer were retrospectively analyzed. All images were collected under HIPAA and IRB approval from a separate multimodality breast imaging clinical trial that has been completed in our department[†]. Only images from the unaffected (*i.e.*, contralateral) breasts were analyzed. DM acquisition was performed with a GE Senographe 2000D FFDM system (GE Healthcare, Chalfont St. Giles, UK). X-ray projections were acquired with spatial resolution of 0.1mm/pixel and 16-bits per pixel gray-levels. Image post-processing was performed with the GE *PremiumView*TM algorithm [11].

2.2. ROI Segmentation

Retroareolar 2.5cm^2 regions of interest (ROI) were segmented from the *PremiumView*TM (GE Healthcare) post-processed images using custom-developed automated software. Briefly, the software implements an edge detection algorithm based on the Hough transform to detect the chest wall in the image [12]. This is followed by the automatic detection of the nipple location as the edge point which is furthest perpendicularly from the chest wall, and the automatic segmentation of a 2.5cm^2 retroareolar ROI behind the detected nipple (Fig.1). Representative ROIs from pre- and post-menopausal women are shown in Figure 2.

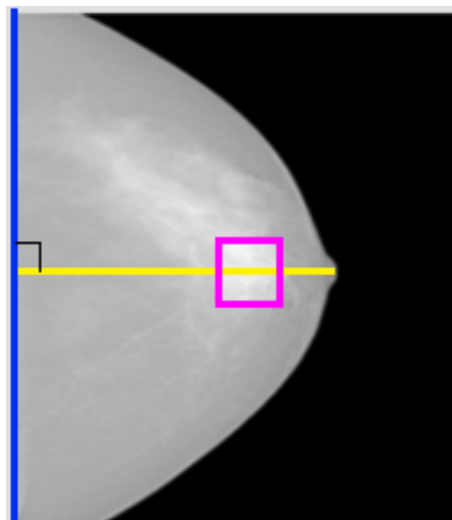


Figure 1: Segmentation of 2.5cm^2 retroareolar region of interest (ROI) (magenta square) based on automated chest wall detection using a Hough transform-based technique (blue) and detection of the nipple using an edge detection algorithm (yellow).

[†] Evaluation of Multimodality Breast Imaging, NIH P01 CA85484, PI: M.D. Schnall

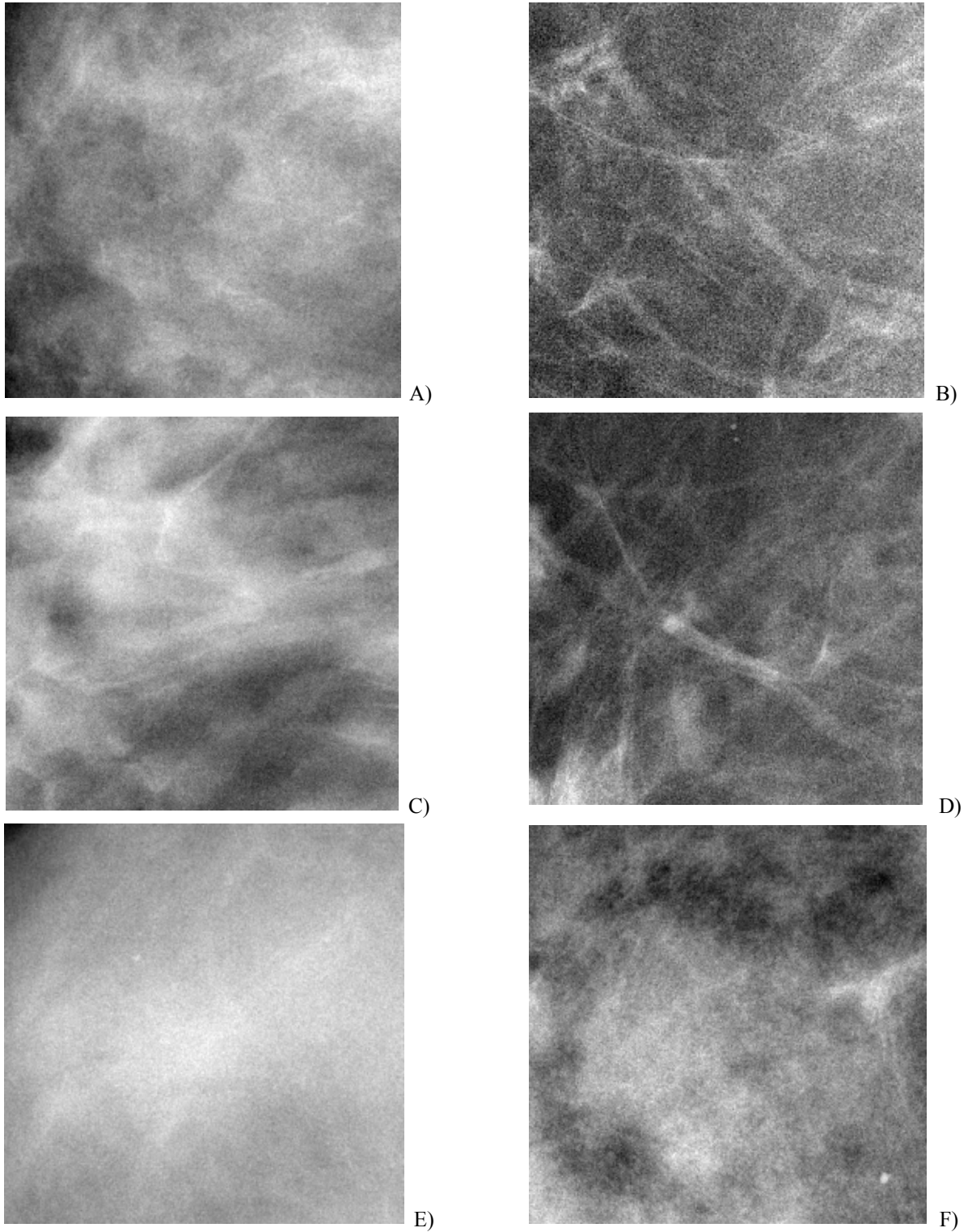


Figure 2. Representative regions of interest (ROIs) from cranio-caudal (CC) digital mammographic images used in our study. The left column A, C and E ROIs represent pre-menopausal cases. The right column B, D and F ROIs represent post-menopausal cases.

2.3. Texture feature extraction

Texture features of skewness, coarseness, contrast, and energy were estimated from all the DM ROIs. These features have been shown in previous studies with mammograms to correlate with the risk of developing breast cancer [12-16].

Skewness reflects the properties of the gray-level histogram and has been used to assess parenchymal density [14, 15]. When the image texture is predominantly composed of fat (*i.e.* the grey-level histogram is skewed to higher values) the skewness tends to be positive, whereas when the texture is primarily formed by dense tissue (*i.e.* the gray level histogram is skewed to lower values) the skewness values tend to be negative. Skewness is the third statistical moment, computed as:

$$skewness = \frac{w_3}{w_2^{\frac{3}{2}}} \quad \text{where}$$

$$w_k = \frac{\sum_{i=0}^{g_{\max}} n_i (i - \bar{i})^k}{N}, \quad N = \sum_{i=0}^{g_{\max}} n_i, \quad \bar{i} = \frac{\sum_{i=0}^{g_{\max}} (in_i)}{N}$$

and n_i represents the number of times that gray level value i takes place in the image region, g_{\max} is the maximum gray-level value and N is the total number of image pixels.

Coarseness is a texture feature that reflects the local variation in image intensity; small coarseness value for an ROI indicates fine texture, where the gray levels of neighboring pixels are different; high coarseness value indicates coarse texture, where neighboring pixels have similar gray level values. Coarseness computation is based on the Neighborhood Gray Tone Difference Matrix (NGTDM) [11, 17] of the gray-level values within the image region.

$$coarseness = \left(\sum_{i=0}^{g_{\max}} p_i v(i) \right)^{-1}, \quad \text{where } v(i) = \begin{cases} \sum |i - \bar{L}_i| \text{ for } i \in \{n_i\} \text{ if } n_i \neq 0 & \text{is the NGTDM} \\ 0 & \text{otherwise} \end{cases}$$

In the above formulas, g_{\max} is the maximum gray-level value, p_i is the probability that gray level i occurs, $\{n_i\}$ is the set of pixels having gray level value equal to i , and \bar{L}_i is given by:

$$\bar{L}_i = \frac{1}{S-1} \sum_{k=-t}^t \sum_{l=-t}^t j(x+k, y+l),$$

where $j(x,y)$ is the pixel located at (x,y) with gray level value i , $(k,l) \neq (0,0)$ and $S=(2d+1)^2$ with d specifying the neighborhood size around the pixel located at (x,y) .

Contrast, Energy, Correlation and Homogeneity, as proposed originally by Haralick [17], require the computation of a gray-level co-occurrence matrix, which is based on the frequency of the spatial co-occurrence of gray-level intensities in the image. Contrast quantifies overall variation in image intensity, while energy is a measure of image homogeneity.

$$contrast = \sum_i \sum_j |i-j|^2 C(i,j), \quad energy = \sum_i \sum_j C(i,j)$$

$$correlation = \frac{\sum_i \sum_j j(i) p(i,j) - \mu_x \mu_y}{\sigma_x \sigma_y}, \quad homogeneity = \sum_{i=0}^{g_{\max}} \sum_{j=0}^{g_{\max}} \frac{C(i,j)}{1+|i-j|}$$

where g is the total number of different gray levels, μ and σ are the mean and standard deviation of the partial probability density function p and C is the normalized co-occurrence matrix [17].

Fractal dimension (FD) was estimated based on the power spectrum of the Fourier transform of the image. The 2D Discrete Fourier Transform (DFT) was performed using the Fast Fourier Transform (FFT) algorithm as:

$$F(u, v) = \sum_{m=0}^{M-1} \sum_{n=0}^{N-1} I(m, n) e^{-j\left(\frac{2\pi}{M}\right)um} e^{-j\left(\frac{2\pi}{N}\right)vn}, \quad u = 0, 1, \dots, M-1 \quad v = 0, 1, \dots, N-1$$

where I is the 2D image region of size (M, N) , and u and v are the spatial frequencies in the x and y directions. The power spectral density P was estimated from $F(u, v)$ as:

$$P(u, v) = |F(u, v)|^2$$

To compute the FD, P was averaged over radial slices spanning the FFT frequency domain. The frequency space was uniformly divided in 24 directions, with each direction uniformly sampled at 30 points along the radial component. To calculate the FD the least-squares-fit of the $\log(P)$ versus $\log(f)$ was estimated, where $f = \sqrt{u^2 + v^2}$ denotes the radial frequency.

The FD is related to the slope β of this log-log plot by:

$$FD = \frac{3D_T + 2 - \beta}{2} = \frac{8 - \beta}{2}$$

where D_T is the topological dimension, and is equal to $D_T=2$ for a 2D image.

2.4. Data analysis

To investigate the association between texture and hormonal activity as indicated by menopause status, receiver operating characteristic (ROC) curve analysis was performed to evaluate feature classification performance between the 72 pre- and the 66 post-menopausal women. The area under the curve (AUC) of the ROC curve was used as an index to evaluate the inherent discriminant capacity of these texture features in differentiating mammographic texture patterns between the two groups.

To assess the collective effect of the combinations of the texture features in distinguishing between pre- and post-menopausal women, a logistic regression model was constructed with menopause as the response variable. The independent effect of each of the texture features on menopause status was investigated. Logistic regression analysis was conducted for each texture feature and their estimated logistic regression coefficients with standard error (SE) were computed. Student's t-test for each partial regression coefficient was used to determine which of the texture features specifically affects the response variable.

ROC curve analysis was performed to assess the classification performance of the logistic regression model in distinguishing between pre- and post-menopausal women. Addition of further variables to the logistic regression model was performed to assess whether the contribution of the mammographic texture variables remains significant in predicting menopause status, after adjusting for potential confounding factors. Specifically, age at menarche, ethnicity, contraception use and hormonal replacement therapy (HRT) use were added to the logistic regression model and the independent contribution of each of the mammographic texture features to the model was assessed using a Student's t-test for each partial regression coefficient.

3. RESULTS

3.1 Texture feature classification performance

ROC feature classification performance shows that all of the texture features, except energy, possess inherent capacity to distinguish between pre- and post-menopausal women (Table 1). The inherent discriminatory capacity of each texture feature in distinguishing between the 72 pre- and the 66 post-menopausal women was assessed using the area under the curve (AUC).

Table 1. Receiver operating characteristic (ROC) curve texture feature classification performance between pre- and post-menopausal women (AUC: area under the curve, S.E.: standard error, CI: confidence interval).

Texture Feature	AUC	S.E.	95% CI		p-value
Coarseness	0.622	0.048	0.529	0.716	0.005
Contrast	0.588	0.049	0.493	0.684	0.034
Grey-Level Spatial Correlation	0.649	0.047	0.557	0.741	0.001
Energy	0.576	0.049	0.480	0.671	0.060
Homogeneity	0.581	0.049	0.485	0.676	0.048
Fractal Dimension	0.613	0.048	0.519	0.707	0.009
Skewness	0.678	0.046	0.589	0.768	0.000

3.2 Logistic Regression Analysis

A logistic regression model that only included texture features yielded three logistic regression coefficients: those of contrast, homogeneity and skewness that significantly affected the model's performance in predicting menopause status ($p < 0.05$). ROC curve analysis to assess the performance of this model in predicting menopausal status yielded an AUC of 0.76 (Fig. 3A).

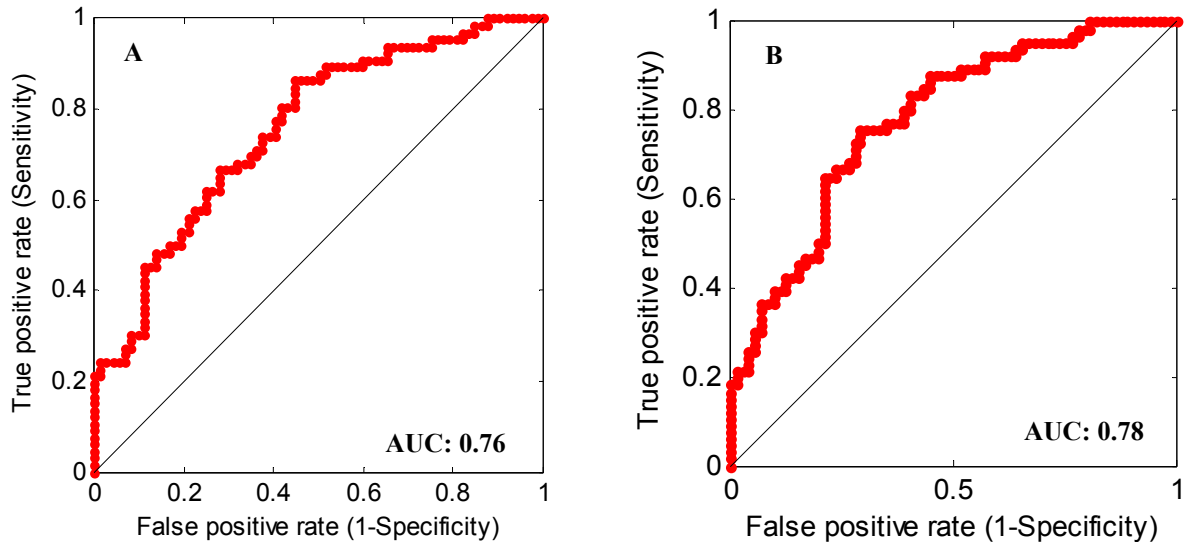


Figure 3. Receiver operating characteristic (ROC) curves for logistic regression including: (A) only texture features and (B) texture features, age at menarche, ethnicity, contraception use and estrogen use. (AUC: area under the curve).

Addition of age at menarche, ethnicity, contraception use and estrogen therapy use lead to a modest improvement to the performance of the model (AUC=0.78) (Fig. 3B), while the texture features maintained significant independent contribution to the model (p -value <0.05). The additional variables considered did not exhibit statistical significance (Table 2).

Table 2. Results for each partial regression coefficient after the addition of further variables to the logistic regression model. P-values are from t-test results for each partial regression coefficient.

	Regression Coefficient	Coefficient P-Values
Model Constant (Intercept)	51.735	0.007
Coarseness	2899.886	0.232
Contrast	-0.009	0.008
Grey-Level Spatial Correlation	-35.131	0.083
Energy	-3225.835	0.803
Homogeneity	-84.505	0.017
Fractal Dimension	-0.935	0.481
Skewness	0.953	0.034
Age at menarche	-0.119	0.429
Estrogen therapy	30.075	1.000
Contraceptive use	-1.090	0.350
Ethnicity	-0.005	0.936

4. CONCLUSION

We performed a study to compare differences in parenchymal texture features between pre- and post-menopausal women. Our results demonstrate that texture features have inherent capacity to distinguish between women's menopausal status. This capacity appears to remain significant independently of potentially confounding variables such as age at menarche, ethnicity, contraception use and estrogen therapy use. The observed differences in parenchymal texture features between pre- and post- menopausal women suggest that mammographic texture patterns may independently reflect endogenous hormonal exposure of the breast tissue. Our long-term goal is to improve breast cancer risk estimation at the individual level by incorporating novel imaging markers of breast tissue composition into breast cancer risk prediction. These texture features could ultimately be incorporated in a breast cancer risk assessment model to aid in cancer risk prediction as surrogate imaging markers of endogenous hormonal activity. Studies are currently underway to validate these findings in a screening population of women.

ACKNOWLEDGEMENT

This work was partially supported by a Department of Defense (DOD) Concept Award (BC086591) and by an American Cancer Society (ACS) Research Scholar Grant (119586-RSGHP-10-108-01-CPHPS). We would also like to thank Dr. Johnny Kuo for developing and maintaining the RSNA Medical Imaging Resource Center (MIRC) image archive.

REFERENCES

1. Parkin DM, Bray F, Ferlay J, Pisani P. Global cancer statistics, 2002. *CA Cancer J Clin* 2005;55:74-108.
2. Group USCSW. United States Cancer Statistics: 1999–2006 Incidence and Mortality Web-based Report. Department of Health and Human Services, Centers for Disease Control and Prevention, and National Cancer Institute 2010.
3. Gulati AP, Domchek SM. The clinical management of mutation carriers. *Curr Oncol Rep* 2008; 10:47-53.
4. Rockhill B, Spiegelman D, Byrne C, Hunter DJ, Colditz GA. Validation of the Gail et al. model of breast cancer risk prediction and implications for chemoprevention. *Journal of the National Cancer Institute* 2001; 93:358-366.
5. Li H, Giger ML, Olopade OI, Lan L. Fractal analysis of mammographic parenchymal patterns in breast cancer risk assessment. *Academic Radiology* 2007; 14:513-521.

6. Li H, Giger ML, Olopade OI, Margolis A, Lan L, Chinander MR. Computerized Texture Analysis of Mammographic Parenchymal Patterns of Digitized Mammograms. *Academic Radiology* 2005; 12:863-873.
7. Huo Z, Giger ML, Olopade OI, et al. Computerized analysis of digitized mammograms of BRCA1 and BRCA2 gene mutation carriers. *Radiology* 2002; 225:519-526.
8. Endogenous Hormones and Breast Cancer Collaborative Group: Endogenous sex hormones and breast cancer in postmenopausal women: Reanalysis of nine prospective studies. *J Natl Cancer Inst* 94:606-616, 2002
9. Zeleniuch-Jacquotte A, Shore RE, Koenig KL, et al: Postmenopausal levels of oestrogen, androgen, and SHBG and breast cancer: Long-term results of a prospective study. *Br J Cancer* 90:153-159, 2004
10. Missmer SA, Eliassen AH, Barbieri RL, et al: Endogenous estrogen, androgen, and progesterone concentrations and breast cancer risk among postmenopausal women. *J Natl Cancer Inst* 96:1856-1865, 2004
11. Kontos D, Bakic PR, Carton AK, Troxel AB, Conant EF, Maidment ADA. Parenchymal texture analysis in digital breast tomosynthesis for breast cancer risk estimation: A preliminary study. *Academic Radiology*. 2009;16(3):283-298.
12. Oliver A, Freixenet J, Mart R, et al. A novel breast tissue density classification methodology. *IEEE Transactions on Information Technology in Biomedicine* 2008; 12:55-65.
13. Harvey JA, Bovbjerg VE. Quantitative Assessment of Mammographic Breast Density: Relationship with Breast Cancer Risk. *Radiology*. 2004;230:29-41.
14. Hartman K, Highnam R, Warren R, Jackson V. Volumetric Assessment of Breast Tissue Composition from FFDM Images. Paper presented at: Digital Mammography (IWDM), 2008.
15. Khazen M, Warren RM, Boggis CR, et al. A pilot study of compositional analysis of the breast and estimation of breast mammographic density using three-dimensional T1-weighted magnetic resonance imaging. *Cancer Epidemiol Biomarkers Prev*. Sep 2008;17(9):2268-2274.
16. Kopans DB. Basic physics and doubts about relationship between mammographically determined tissue density and breast cancer risk. *Radiology*. Feb 2008;246(2):348-353.
17. McCormack VA, dos Santos Silva I. Breast density and parenchymal patterns as markers of breast cancer risk: a meta-analysis. *Cancer Epidemiology, Biomarkers & Prevention*. 2006;15(6):1159-1169.